Structural and Functional Characterization of EMF10, a Heterodimeric Disintegrin from *Eristocophis macmahoni* Venom That Selectively Inhibits α5β1 Integrin[†,‡]

Cezary Marcinkiewicz,[§] Juan J. Calvete,[||] Senadhi Vijay-Kumar,[§] Mariola M. Marcinkiewicz,[§] Manfred Raida,[⊥] Paul Schick,[○] Roy R. Lobb,[▽] and Stefan Niewiarowski*[,§]

Department of Physiology, Sol Sherry Thrombosis Research Center, Fels Research Institute for Cancer and Molecular Biology, Temple University, School of Medicine, 3400 North Broad Street, Philadelphia, Pennsylvania 19140, Instituto de Biomedicina, CSIC, Valencia, Spain, Institute of Peptide Research, Hannover, Germany, Cardeza Foundation for Hematological Research, Thomas Jefferson University, Philadelphia, Pennsylvania 19107, and Biogen Inc., Cambridge, Massachusetts 02142

Received March 24, 1999; Revised Manuscript Received August 6, 1999

ABSTRACT: α5β1, a major fibronectin receptor, is a widely distributed integrin that is essential for cell growth and organ development. Here, we describe a novel heterodimeric disintegrin named EMF10, isolated from the *Eristocophis macmahoni* venom, that is an extremely potent and selective inhibitor of α5β1. EMF10 inhibited adhesion of cells expressing α5β1 to fibronectin (IC_{50} = 1−4 nM) and caused expression of a ligand-induced binding site (LIBS) on the β1 subunit of α5β1 integrin. It partially inhibited adhesion of cells expressing αIIbβ3, αvβ3, and α4β1 to appropriate ligands only at concentration higher than 500 nM. Guinea pig megakaryocytes expressing α5β1 adhered to immobilized EMF10 and showed extensive spreading and cytoskeletal mobilization. As determined by electrospray mass spectrometry, EMF10 is composed of two species with molecular masses of 14 575 and 14 949 Da, respectively. EMF10 is a heterodimer containing two subunits: EMF10A (M_r 7544 Da) and EMF10B (M_r 7405 and 7032 Da) linked covalently by S−S bonds. Subunit B showed heterogeneity and may be present as EMF10B1 (M_r 7032) and EMF10B2 (M_r 7405). In putative hairpin loops, EMF10A and EMF10B contained CKKG**RGD**NLNDYC and CWPA**MGD**WNDDYC motifs, respectively. The reduced and alkylated subunit B of EMF10 inhibited adhesion of K562 cells to fibronectin in a dose-dependent, saturable manner with IC_{50} of 3 μM. The synthetic, cyclic CKKG**RGD**NLNDYC and CWPA**MGD**WNDDYC peptides expressed their inhibitory activity in the same system with IC_{50} of 100 μM. We propose that α5β1 recognition of EMF10 is associated with the MGDW motif located in a putative hairpin loop of the B subunit and that the expression of activity may also depend on the RGDN motif in the subunit A and on the C-termini of both subunits.

α5β1, a major fibronectin receptor, is a widely distributed integrin that is essential for cell growth and organ development (*1*). The knockout mice in which α5 or β1 genes are deleted do not survive beyond the early fetal stage (*2*). Other studies indicate that this integrin plays a significant role in cell growth and cancer metastases (*3*). Integrin α5β1 mediates elimination of amyloid β peptide and may protect neuronal cells against apoptosis, which is an essential event in the course of the Alzhemer disease (*4*). It has been found that α5β1-mediated adhesion up-regulated the anti-apoptosis protein Bcl-2 (*5*), and it activates the signaling protein ShC (*6*). α5β1 is an RGD-dependent receptor, but in contrast to αvβ3, it binds weekly to short RGDX peptides. Using phage libraries, Koivunen et al. (*7, 8*) identified a number of short peptides that inhibit α5β1 at micromolar concentrations. The cyclic cRRETAWAc peptide obtained by chemical synthesis (*9*) can be coupled to agarose and used for α5β1 purification.

Most recently, we isolated in our laboratory a dimeric disintegrin EC3 from *Echis carinatus suchoreki* venom (*10*). This disintegrin contains 10 cysteines in each subunit, and its molecular mass amounts to 14 761 Da. EC3 is a strong inhibitor of α4β1 and α4β7 and a weak inhibitor of α5β1 and platelet aggregation. RGD motif is substituted in the subunit A by VGD and in the subunit B by MLD motifs, respectively. The present study identifies a new member of the heterodimeric disintegrin family, named EMF10. EMF10, isolated from *Eristocophis macmahoni* venom, is a several-fold more potent inhibitor of α5β1 binding to fibronectin than any other compound reported in the literature. Our data

[†] Aided in part by grants from American Heart Association Southeastern Pennsylvania Chapter (S.N.), American Diabetes Association (S.N.), Barra Foundation (S.N.), Initial Investigator grant from American Heart Association (C.M.), and NIH HL51481 (P.S.).

[‡] The EMF10A and EMF10B amino acid sequences have been deposited in Swiss Protein (SWISS-PROT) Databank with the assignment numbers P81742 and P81743.

* To whom all correspondence should be addressed. Tel: 215-707-4408. Fax: 215-707-4003. E-mail: stni@astro.temple.edu.

[§] Temple University.

[||] Instituto de Biomedicina.

[⊥] Institute of Peptide Research.

[○] Thomas Jefferson University.

[▽] Biogen Inc.

[1] Abbreviations: ep, ethylpyridylated; Ig, immunoglobin; VCAM-1, vascular cell adhesion molecule 1; MadCAM-1, mucosal addressin cell adhesion molecule 1; VLA4, very late antigen 4; VLA5, very late antigen 5; HPLC, high-performance liquid chromatography; HBSS, Hanks' balanced salt solution; BSA, bovine serum albumin; CMFDA, 5-chloromethylfluoresceine acetate; CHO cells, Chinese hamster ovary cells; LIBS, ligand-induced binding site; MK, megakaryocytes; DPBS, Dulbecco's phosphate-buffered saline.

10.1021/bi9906930 CCC: $18.00
Published on Web 09/17/1999

also suggest that a novel motif CWPAMGDWNDDYC is important for $\alpha5\beta1$ recognition.

EXPERIMENTAL PROCEDURES

Materials. Monoclonal antibodies HP2/1 (anti-$\alpha4$ subunit of VLA4[1]), SAM-1 (anti-$\alpha5$ subunit of VLA5), and Lia 1/2 (blocking, anti-$\beta1$ subunit) were purchased from Immunotech, Inc. (Westbrook, ME); 9EG7 (anti-LIBS in $\beta1$ integrin) (*11*) was purchased from Pharmingen (San Diego, CA); and mab 62 (anti-LIBS in $\beta3$ integrin) was generously provided by Dr. Mark Ginsberg (Scripps Research Institute). Recombinant human VCAM-1 (*12*) was a gift from Dr. M. Renz (Genentech, San Francisco, CA); recombinant MadCAM was from Biogen, Inc. Vitronectin and fibronectin were purchased from Calbiochem (La Jolla, CA) and Sigma (St. Louis, MO), respectively. GRGDSP and GRGESP peptides were purchased from Bachem (Torrance, CA). Echistatin and eristostatin were isolated from *Echis carinatus suchoreki* and *Eristocophis macmahoni* venom, respectively, as described earlier (*13*).

Cell Lines. A5 and VNRC3 cells, CHO cells transfected with human $\alpha IIb\beta3$ and $\alpha v\beta3$ integrins, respectively (*14*), were kindly provided by Dr. M. Ginsberg (Scripps Research Institute, La Jolla, CA). RPMI 8866 cells were a gift from Dr. A. Garcia-Pardo (Madrid, Spain), and K562 cells transfected with $\alpha6$ integrin were a gift from Dr. A. Sonnenberg (Netherlands Cancer Institute, Amsterdam, Holland). Cells transfected with $\alpha2$ were from Dr. M. Hemler (Dana Farber Cancer Institute, Boston, MA). Jurkat cells, Ramos cells, and K562 cells were purchased from ATCC (Rockville, MD).

Purification of EMF10. Lyophilized *E. macmahoni* venom obtained from Latoxan Serpentarium (Rosans, France) was dissolved in 0.1% trifluoroacetic acid (30 mg/mL). The solution was centrifuged for 5 min at 5000 rpm to remove the insoluble proteins. The pellet was discarded, and the supernatant was applied to a C-18 HPLC column (Hesperia, CA). The column was eluted with an acetonitrile linear gradient 0−80% over 45 min. This yielded eristostatin, a potent inhibitor of $\alpha IIb\beta3$ in fraction 7 (*13*) and EMF10, a potent inhibitor of $\alpha5\beta1$, in fraction 10. (EMF10 is an abbreviation of *E. macmahoni* fraction 10). EMF10 eluted at approximately 40% of acetonitrile was collected and lyophilized and then dissolved in water. The received solution was re-injected to the same HPLC column; however, more "flat" gradient of acetonitrile was applied (0−60% over 45 min). The main peak containing EMF10 was collected and lyophilized. Purity of EMF10 was tested by SDS−PAGE and mass spectrometry. The overall yield of EMF10 was about 8 mg from 1 g of crude venom.

Separation of Ethylpyridylated EMF10 Subunits. Reduction and ethylpyridylation of EMF10 was performed according to the procedure used before for trigramin (*15*). Briefly, 100 μg of EMF10 was incubated in 200 μL of 6 M guanidine hydrochloride, 4 mM EDTA, 0.1 M Tris-HCl, pH 8.5, and 3.2 mM dithiothreitol for 2 h in the dark at room temperature, followed by the addition of 2 μL of 4-vinylpyridine. Modified subunits EMF10A and EMF10B were isolated by reversed-phase HPLC on a C-18 column with acetonitrile gradient 0−80% over 45 min.

Structural Characterization of EMF10. N-terminal sequence analyses were done with an Applied Biosystems Precise instrument following the manufacturer's instructions. Amino acid analyses (after sample hydrolysis with 6 N HCl for 24 h at 110 °C) were performed with a Pharmacia AlphaPlus analyzer. For quantitation of sulfydryl groups, native EMF10 (2 mg/mL) in 100 mM Tris·HCl, pH 9.0, 150 mM NaCl, 6 M guanidine hydrochloride) was heat-denaturated (1 min at 100 °C), cooled at room temperature, and treated with iodoacetoamide (10-fold molar excess over total cysteine content, determined by amino acid analysis) for 1 h at room temperature. Carboxymethylcysteine was determined by amino acid analysis. The molecular masses of native EMF10 and HPLC-isolated ethylpyridylated subunits were determined by electrospray ionization mass spectrometry using a Sciex API-III triple quadruple LC-MS/MS mass spectrometer.

Ethylpyridylated (ep) EMF10A (2−5 mg/mL in 100 mM ammonium bicarbonate, pH 8.6, containing 1 M guanidine hydrochloride) was digested with endoproteinase Lys-C (Boehringer Mannheim, Germany) with an enzyme:substrate ratio of 1:250 (w/w) for 18 h at 37 °C. Peptides were separated by reversed-phase HPLC on Lichrosphere (Merck, Germany) RP-100 C18 (4 × 250 mm, 5 μm particle size) column eluting at 1 mL/min with a mixture of TFA in water (solution A) and acetonitrile (solution B). Chromatographic conditions were as follows: isocratic (5% B) for 5 min, followed by 5−35% B for 70 min, and 35−70% B for 30 min. Chromatographic fractions were monitored at 220 nm and collected manually. ep-EMF10B (10 mg/mL in 70% (v/v) formic acid) was degraded with CNBr (100 mg/mL final concentration) overnight at room temperature in tubes sealed under N_2 atmosphere and protected from the light. The reaction mixture was dried in a SpeedVac and dissolved in 5% (v/v) formic acid. Peptides were isolated by reversed-phase HPLC as above, using the following chromatographic conditions: isocratic (5% B) for 5 min, followed by 5−40% B for 70 min, and 40−70% B for 25 min.

Polypeptide Synthesis. The 13-amino acid peptides cyclized through Cys−Cys residues were synthesized by assembling on 4-benzylxybenzyl alcohol resin on automated peptide synthesizer (*16*). Piperidine/toluene was used for removal of N^a-9-fluorenylmethyloxycarbonyl (Fmoc) group. Neutralization and coupling were carried out in *N*-methylpyrrolidinone. The benzotriazole-*N*,*N*,*N*′,*N*′-tetramethyluronium hexafluorophosphate (HBTU)/1-hydroxybenzotriazole mediated coupling efficiency by a quantitative ninhydrin analysis. Removal of the side-chain protecting groups and cleavage of the assembled peptide from the resin were achieved by treating with TFA in the presence of ethane dithiol, crystalline phenol, thioanisole, and triisopropyl silane as scavengers. The peptides were purified using HPLC on C18 column with a water/acetonitrile gradient, containing 0.1% TFA. The amino acid composition of the peptides was determined by the Pico Tag method. The molecular mass of the peptides was confirmed using mass spectrometry.

Adhesion Studies. Adhesion of cultured cells labeled with 5-chloromethylfluorescein diacetate (CMFDA) was performed as described earlier (*17*). Briefly, disintegrins, fibronectin, VCAM-1, or MadCAM were immobilized on a 96-well microtiter plate (Falcon, Pittsburgh, PA) in PBS buffer overnight at 4 °C. Wells were blocked with 1% BSA in HBSS buffer. Cells were labeled with fluorescein by incubation with 12.5 μM CMFDA in HBSS buffer containing

1% BSA at 37 °C for 15 min. Unbound label was removed by washing using the same buffer. Labeled cells (1×10^5 per sample) were added to the well in the presence or absence of inhibitors and incubated at 37 °C for 30 min. Unbound cells were removed by aspiration, the wells were washed, and bound cells were lysed by adding 0.5% Triton X-100. In parallel, the standard curve was prepared in the same plate from a known concentration of labeled cells. The plate was read using a Cytofluor 2350 fluorescence plate reader (Millipore, Bedford, MA) at 485 nm EX (excitation) filter and 530 nm EM (emission) filter.

Expression of LIBS (Ligand-Induced Binding Site Epitope). 9EG7, anti-LIBS monoclonal antibody recognizing β1 integrin (*18*), was immobilized on the 96-wells microtiter plate (0.5 μg/well), in PBS buffer, overnight at 4 °C. K562 cells were labeled with CMFDA, and adhesion of these cells was measured in the presence or absence of various concentrations of disintegrins. We accepted that the enhancement of cell adhesion reflected expression of LIBS epitope interaction with monoclonal antibody. The epitope recognized by 9EG7 mab is located on β1 subunit, and in $\alpha 5\beta 1$ integrin it is sensitive to Ca^{2+} cations (*11, 18*). For this reason, it was difficult to select appropriate calcium milieu that does not interfere with antibody binding and would support disintegrin binding. Satisfactory results were obtained after immobilization of 9EG7 on plastic. 9EG7 after immobilization still did not bind K562 cells in the presence of calcium; however, the addition of EMF10 or echistatin strongly promoted this adhesion.

Adhesion of Guinea Pig Megakaryocytes and Demonstration of Cytoskeletal Changes by Confocal Microscopy. Guinea pig megakaryocytes (MK) were isolated from bone marrow, washed, and resuspended in Dulbecco's phosphate-buffered saline (DPBS) containing calcium and magnesium (*19*). The purity was about 90% by cell size and >98% by protein content. Aliquots of MK (2×10^4/100 μL) were incubated for 30 min at 37 °C on triplicate coverslip coated with gelatin (1%) followed by bovine plasma fibronectin or EMF10 (50 μg/mL). The coverslips were washed with DPBS and the MK were fixed with 3.7% formaldehyde (20 min) and permeabilized with 0.25% Triton X-100 (10 min). After being washed with PBS, the MK were incubated (30 min at 37 °C) in turn with 5% goat serum, rabbit anti-human α-actin antibody, and FITC-labeled goat anti-rabbit IgG. The coverslips were mounted over fluorescence-preserving glycerol-PBS mounting solution and visualized with a Bio-Rad MRC-600 krypton−argon laser confocal microscope adapted to Zeiss Axiovert 100 inverted microscope equipped with a Zeiss 63X Plan Apo lens.

RESULTS

Purification of EMF10 Subunits. Electrospray ionization mass spectrometric analysis of native EMF10 yielded two isotope-averaged molecular ions of 14 575 ± 1.5 Da and 14 947 ± 3.5 Da. After reduction and alkylation with vinylpyridine, EMF10 separated into two subunits, referred to as EMF10A and EMF10B (Figure 1). ep-EMF10A and ep-EMF10B eluted from the HPLC column at about 39.2% and 48% acetonitrile, respectively. The molecular mass of ep-EMF10A was 8604 ± 1 Da. epEMF10B displayed two molecular ions of two isotope-averaged molecular masses

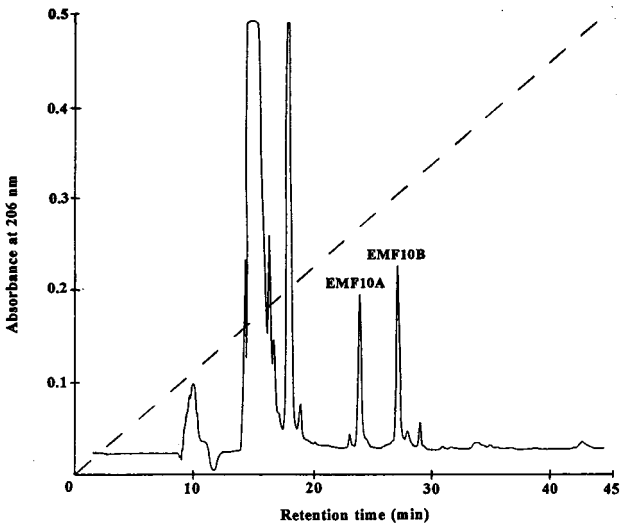

FIGURE 1: Separation of reduced and ethylpyridylethylated EMF10 subunits by reverse-phase HPLC. Purified EMF10 (100 μg) was reduced and alkylated by incubation with 6 M guanidine hydrochloride, 4 mM EDTA, 0.1 M Tris-HCl, pH 8.5, 3.2 mM dithiothreitol, and 2 μL of 4-vinylpyridine for 2 h at room temperature. The mixture was applied on HPLC, and elution was performed with a linear gradient of acetonitrile from 0 to 80% at a flow rate 2.0 mL/min.

of 8092 ± 0.5 and 8465 ± 3.5 Da. This result indicated that EMF10 was a mixture of two heterodimers composed of a common A subunit and disulfide-linked to either EMF10B1 or EMF10B2. Amino acid analysis of iodoacetamide-treated EMF10 showed that it did not contain free sulfydryl groups. On the other hand, amino acid analyses of ep-EMF10A and ep-EMF10(B1 + B2) indicated that each EMF10 subunit contained 10 cysteine residues per molecule. Thus, the molecular masses calculated for the reduced EMF10A, EMF10B1, and B2 polypeptides were 7554, 7042, and 7409 Da, respectively. The molecular mass of two EMF10 heterodimers (A−B1: 7554 + 7041−20) and (A−B2: 7554 + 7409−20) amounted to 14 575 and 14 944, respectively. Each heterodimer contained 20 cysteines.

Amino Acid Sequence and Subunit Composition of EMF10. N-terminal sequence analysis of native EMF10 showed two sequences in equimolar amounts, which after sequencing of HPLC-isolated subunits were interpreted as MNSANPCCD-PITCKPKKGEHCVSGPC (EMF10A) and ELLQNSGNPC-CDPVTCKPRRGEHCVS (EMF10B1 + B2). The complete amino acid sequences of the EMF10 A and B subunits were determined by N-terminal sequence analyses of whole subunits and peptides released following digestion (Figure 2). EMF10A displayed a single 69-residue amino acid sequence, including 10 cysteines. The calculated isotope-averaged molecular mass of reduced EMF10A is 7553.6 Da. Amino acid sequencing of EMF10B revealed a 68-residue polypeptide with 10 cysteine residues and showed a heterogeneity at position 35 (F/K). The isotope-averaged molecular mass of EMF10B2, which has K35 and 68 residues is 7408.4 Da. The molecular mass of EMF10B1, composed of 64 residues, with phenylalanine at position 35, is 7040.9 Da. Four amino acids (PVFK) at the C-terminus are missing. These data demonstrated that EMF10B1 and EMF10B2 differ only in one amino acid residue and in the length of their polypetide chains.

FIGURE 2: Amino acid sequence of EMF10 subunits. The amino acid sequences of EMF10A and EMF10B were established by N-terminal sequencing of reduced and ethylpyridylthylated subunits and by sequencing peptides isolated from digest with endoproteinase Lys-C (EMF10A) or digest with CNBr (EMF10B).

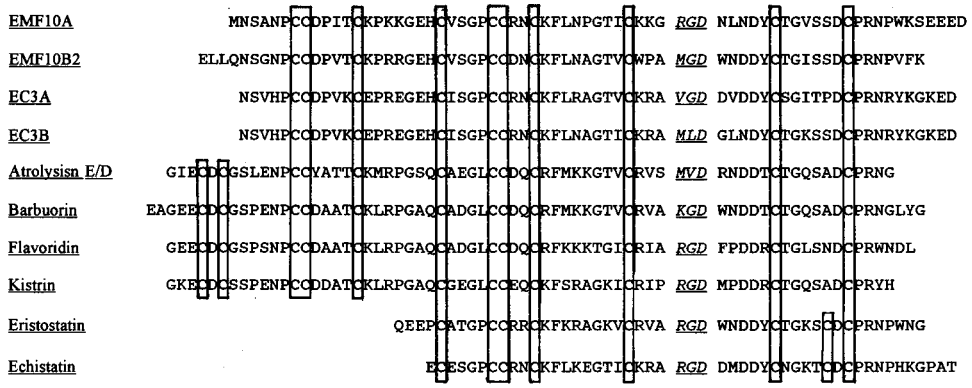

FIGURE 3: Comparison of amino acid sequences of EMF10A and EMF10B with other disintegrins. The cysteines are boxed. Echistatin (*31*) and eristostatin (*22*) represent short disintegrins. Kistrin (*32*), flavoridin (*33*), barbourin (*34*), and atrolysin E/D (*35*) represent medium size disintegrins. EC3 (*10*) is a heterodimeric disintegrin.

EMF10 subunits showed a high degree of sequence similarity with subunits of heterodimeric disintegrin EC3 and with monomeric disintegrins of various length including flavoridin, kistrin, eristostatin, and echistatin (Figure 3). The highest degree of similarity was found between EMF10 subunits and eristocophin I and II, the peptides isolated by Siddiqi et al. (*20*) from reduced venom of *E. macmahoni*. EMF10A and eristocophin I showed identical amino acid sequences except for an additional seven amino acids at the C-terminus of EMF10A. The N-terminal sequence of EMF10B (1 and 2) (ELLQNSGNPCC...) was longer than the corresponding sequence of eristocophin II (ESAGPCC...), and EMF10B displayed additional three C-terminal residues (VFK). Each subunit of EMF10 contained 10 highly conserved cysteines showing the same alignment as the 10 cysteines in EC3 subunits (*10*), whereas monomeric disintegrins contain 8, 12, or 14 cysteines. The RGD motif is present in most monomeric disintegrins except for barbourin where it is substituted with KGD and in atrolysin E/D where it is substituted with MVD (Figure 3). Only the aspartic acid is highly conserved in each disintegrin. Interestingly, the RGD motif is present only in subunit A of EMF10, and it is substituted with MGD in subunit B. An unusual feature of subunit B is that it contains two tryptophans in its putative hairpin loop. It should be noticed that other disintegrins contain at the most one tryptophan in their loops.

Effect of EMF10 on the Integrins Interaction with Their Ligands. EMF10 is a very strong inhibitor of the $\alpha5\beta1$ integrin. Its ability to inhibit adhesion of cells expressing $\alpha5\beta1$ to fibronectin was higher than that of other known disintegrins (Table 1). For instance echistatin was 5-fold less active than EMF10 in this assay system, whereas it was over 12-fold more active in inhibiting ADP-induced platelet aggregation. Accordingly, EMF10 was 10- and 100-fold less active than echistatin in inhibiting adhesion of αIIb$\beta3$ expressing cells (A5) to fibrinogen and $\alpha v\beta3$ expressing cells (VNRC3) to vitronectin, respectively. None of the disintegrins tested inhibited adhesion of K562 cells transfected with $\alpha6$ integrin to immobilized laminin. EMF10 inhibited adhesion of resting guinea pig megakaryocytes to fibronectin with $IC_{50} = 1$ nM, being at least 10-fold more potent than echistatin. EMF10 inhibited K562 cells binding to fibronectin at a concentration about 2 orders of magnitude lower than the concentration required to inhibit adhesion of cells expressing $\alpha4\beta1$ integrin (Ramos and Jurkat cells) to immobilized VCAM-1. Interestingly, EMF10 inhibited more strongly adhesion of Ramos cells to immobilized VCAM-1 than that of Jurkat cells. Monoclonal antibody against $\alpha5$ (SAM-1) completely inhibited binding of Jurkat cells to immobilized EMF10 at a concentration of 10 μg/mL. HP2/1 monoclonal antibody (anti-$\alpha4$) at the same concentration did not compete with EMF10 for Jurkat cells binding. Binding of EMF10 to Jurkat cells was RGD-dependent. GRGDSP peptide at 1 mM concentration partially inhibited adhesion of Jurkat cells to immobilized EMF10. Control GRGESP peptide did not inhibit this binding (Figure 4).

LIBS Expression on $\beta1$ Integrin by Disintegrins. Echistatin, EC3, and EMF10 significantly increased adhesion of K562

Table 1: Comparison of the Inhibitory Effects of EMF10, Echistatin, and Eristostatin on Various Integrins[a]

cell suspension	integrin	ligand	assay	IC_{50} (nM)		
				EMF10	echistatin	eristostatin
Platelets	αIIbβ3	Fg	ADP−PA	1 600	130	59
A5 (CHO αIIbβ3)	αIIbβ3	Fg	CA	500	50	5
VNRC3 (CHOαvβ3)	αvβ3	Vn	CA	5 000	50	>10 000
K562	α5β1	Fn	CA	4	20	>10 000
K562 (α6)	α6β1	Lm	CA	>10 000	>10 000	>10 000
K562 (α2)	α2β1	Coll	CA	>10 000	>10 000	>10 000
Jurkat	α4β1	VCAM-1	CA	2 000	>10 000	>10 000
Ramos	α4β1	VCAM-1	CA	560	>10 000	>10 000
RPMI 8866	α4β7	MadCAM	CA	>10 000	>10 000	>10 000
GPRmk	α5β1	Fn	CA	1	10	ND

[a] The data represent mean from three duplicated experiments. Fg, fibrinogen; Fn, fibronectin; Vn, vitronectin; Lm, laminin; coll, collagen 1; PA, platelet aggregation; CA, cell adhesion; GPRmk, guinea pig resting megakaryocytes; ND, not determined.

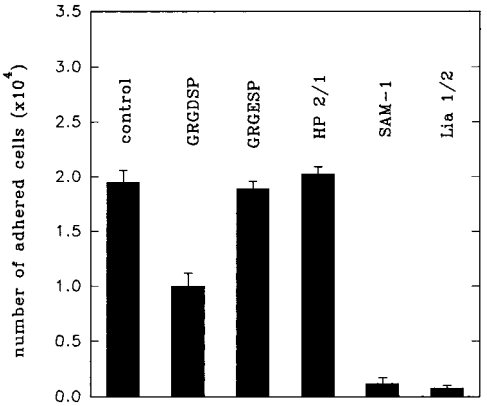

FIGURE 4: Effect of RGD peptides and monoclonal antibodies on Jurkat cells/EMF10 interactions. Adhesion study was performed using CMFDA-labeled Jurkat cells in the absence (control) or the presence of 1 mM GRGDSP or GRGESP peptides and 10 μg/mL HP 2/1, SAM-1, and Lia 1/2 monoclonal antibodies. Error bars represent SD from three duplicated experiments.

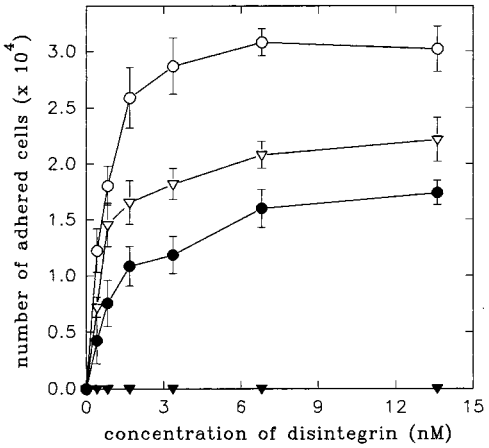

FIGURE 5: Effect of EMF10, echistatin, and eristostatin on adhesion of K562 cells to immobilized 9EG7 monoclonal antibody. The 9EG7 monoclonal antibody (0.5 μg/well) was immobilized on 96-well plate overnight at 4 °C in PBS buffer. The CMFDA-labeled cells were added in the absence (control) or the presence of different concentrations of EMF10 (open circles), echistatin (open triangles), EC3 (filled circles), and eristostatin (filled triangles). Adhesion was performed as described in Experimental Procedures. Error bars represent SD from three duplicated experiments.

cells to immobilized 9EG7, an anti-LIBS monoclonal antibody. This effect saturated at about 8 nM concentration for all three disintegrins; however, the total number of adhering cells was the highest in experiment with EMF10, about 40% lower in experiment with echistatin, and 50% lower in experiment with EC3. Eristostatin, which does not interact with α5β1, did not increase the binding of K562 cells to immobilized 9EG7 mab (Figure 5). EMF10 did not induce LIBS epitope in CHO cells transfected with β3 integrins (data not shown) in contrast to echistatin and eristostatin, which showed a strong LIBS induction (*13*, *21*).

Adhesion of Guinea Pig Megakaryocytes to Immobilized EMF10 and Fibronectin and Cytoskeletal Changes. EMF10 inhibited adhesion of resting guinea pig megakaryocytes to immobilized fibronectin (Table 1, ref *19*). The guinea pig megakaryocytes adhering to immobilized EMF10 and fibronectin on the coverslips were observed under confocal fluoresence microscopy (Figure 6). As demonstrated by staining of permeabilized cells with anti-α actinin antibody, the adhesion of cells to both ligands resulted in blebbing and pseudopods formation, suggesting cytoskeletal mobilization. Blebbing did not occur in megakaryocytes adhering to polylysine as shown previously (*19*). These data suggest that α5β1 interaction with immobilized EMF10 leads to intracellular signaling.

Effect of Isolated EMF10 Subunits and Synthetic Peptides on the Adhesion of K562 Cells to Immobilized Fibronectin. EMF10 subunits separated as shown in Figure 1 were tested for the inhibition of K562 cells adhesion to fibronectin (Figure 7). Despite reduction and alkylation these subunits remained active, although their activity was decreased by about 1000-fold. EMF10B inhibited K562 cell adhesion in a dose-dependent manner reaching 100% inhibition at 14 μM. At the same range of concentrations, EMF10A caused only a partial (20%) inhibition of K562 cell adhesion to fibronectin. As a negative control the alkylated kistrin was used. This medium size monomeric disintegrin has a similar molecular mass to EMF10 subunits, and it does not inhibit adhesion of K562 cells to fibronectin (Marcinkiewicz et al., unpublished observation). To evaluate a role of RGD and MGD motifs in the inhibitory activity of EMF10, we synthesized cyclic peptides patterned on the putative hairpin loop of EMF10A and EMF10B. Both peptides inhibited adhesion of K562 cells to immobilized fibronectin in a dose-dependent manner with IC_{50} for *CKKG**RGD**NLNDYC* and *CWPA**MGD**WNDDYC* amounting to 101.9 ± 1.8 and 163 ± 42 μM, respectively (Figure 8). As a negative control, the activity of cyclic *CKKG**RGA**NLNDYC* and *CWPA**MGA**WNDDYC* was tested. Both peptides showed no activity confirming a former observation about the

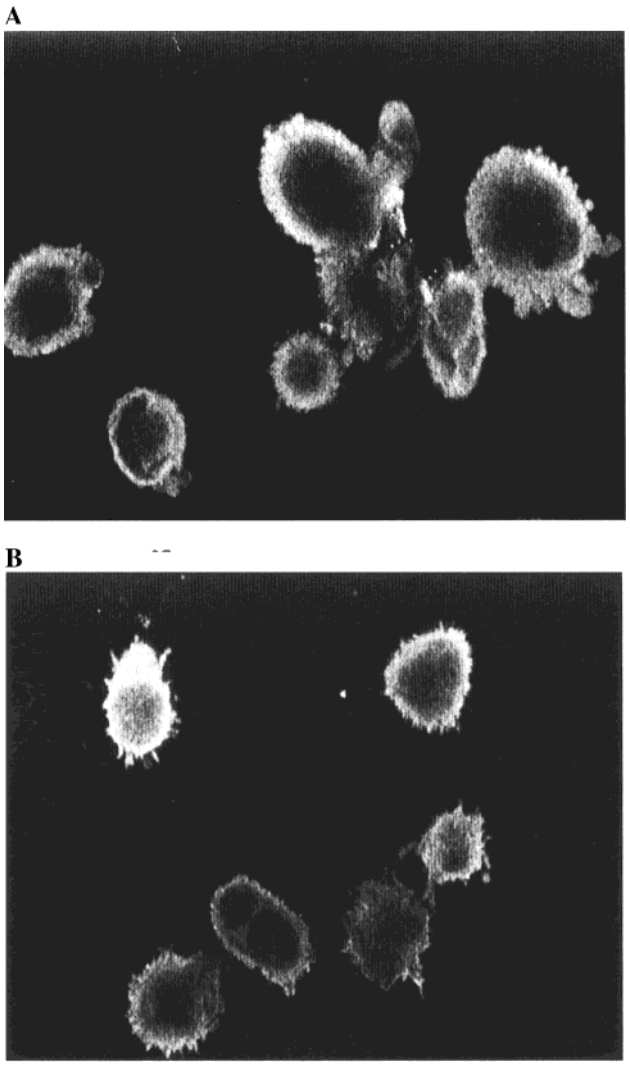

FIGURE 6: Adhesion of guinea pig megakaryocytes to immobilized EMF10 and fibronectin. Isolated guinea pig megakaryocytes layered on cover slips coated with fibronectin or EMF10. The cells were permeabilized with 0.25% Triton X-100, incubated with anti-α-actin antibody and FITC-labeled goat anti-rabbit IgG, and examined by confocal microscopy. Panels A and B demonstrate megakaryocytes adhesion to fibronectin and EMF10, respectively.

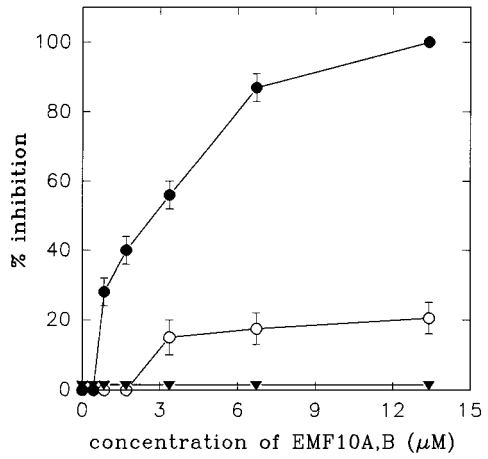

FIGURE 7: Effect of reduced and alkylated EMF10A and EMF10B on adhesion of K562 cells to immobilized fibronectin. The experiment was performed as described in the legend to Figure 2 using different concentrations of EMF10A (open circles) and EMF10B (filled circles). As a negative control, the alkylated kistrin was used (open triangels). Error bars represent SD from three duplicated experiments.

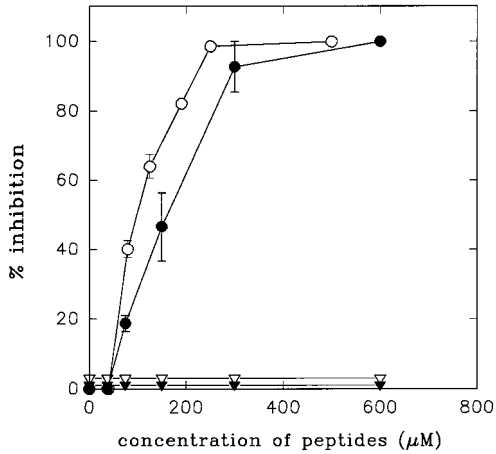

FIGURE 8: Effect of EMF10A and EMF10B derived peptides on K562 cells adhesion to immobilized fibronectin. The experiment was performed as described in the legend to Figure 2. Inhibitory effect of cyclic *CKKGRGDNLNDYC* (EMF10A) and *CWPAMGDWNDDYC* (EMF10B) peptides is shown by open circles and filled circles, respectively. As a negative control, the cyclic *CKKGRGANLNDYC* (open triangels) and *CWPAMGAWNDDYC* (filled triangels) peptides were used. Error bars represent SD from three duplicated experiments.

importance of aspartic acid in the RGD or related disintegrin motifs. This residue is conserved in all disinintegrins.

DISCUSSION

This paper describes identification, isolation, and characterization of a novel heterodimeric disintegrin from *E. macmahoni* venom. This disintegrin, named EMF10, resembles another heterodimeric disintegrin (EC3 from *Echis carinatus*) recently discovered and characterized in our laboratory. Both disintegrins have similar molecular weights of about 14.5 kDa and are composed of two subunits, each containing 65−70 amino acids. Each of these four subunits contains 10 cysteines.

Two peptides, eristocophin I and II, isolated by Siddiqi et al. (*20*) from the reduced venom of *E. macmahoni* appear to represent degradation products of EMF10. Eristocophin I corresponds to EMF10A with seven amino acid residues truncated at the C-terminus. Eristocophin II is highly similar to EMF10B. These proteins differ in length and in their N-terminal sequences. N-terminal sequences of EMF10B and eristocophin II are ELLQNSGNPCC and ESAGPCC, respectively. However, the biological activity of eristocophin I and II has not been reported.

EC3 and EMF10 show a high degree of amino acid sequence similarity with viper venom monomeric disintegrins such as echistatin, kistrin, and flavoridin (*22*, *23*), including identical alignment of conserved cysteines. In view of the fact that EMF10 does not express any free cysteine we propose, that eight cysteines of each subunit are involved in the formation of four intramolecular bridges and that four cysteines are involved in the formation of two intermolecular bridges between subunits A and B. The intermolecular S−S bridges are formed between cysteine 8 of EMF10 A and cysteine 11 of EMF10B and between cysteine 12 of EMF10A and cysteine 16 of EMF10B (Calvete et al.; manuscript submitted). The pattern of intramolecular S−S bonds in

EMF10A and B is the same like in disintegrin flavoridin (*24*, *25*) and kistrin (*26*).

Considering a high degree of amino acid sequence similarity between EC3 and EMF10, one can suggest that both heterodimeric disintegrins have the same pattern of intra- and intermolecular S−S bonds. Both EC3 and EMF10 are antagonists of $\beta1$ integrin and inhibit weakly $\alpha v\beta3$ and $\alpha IIb\beta3$ integrin. The major difference between both heterodimeric disintegrins is different reactivity with $\alpha4\beta1$, $\alpha5\beta1$, and $\alpha4\beta7$ integrins. EC3 strongly inhibits adhesion of cells expressing $\alpha4\beta1$ to immobilized VCAM-1 (IC_{50} = 20−30 nM) and cells expressing $\alpha4\beta7$ to immobilized MAdCAM-1 (IC_{50} = 6−10 nM), and it is rather a weak inhibitor of K562 cells expressing $\alpha5\beta1$ to immobilized fibronectin (IC_{50} = 150 nM). On the other hand, EMF10 inhibits weakly adherence of cells expressing $\alpha4\beta1$ to immobilized VCAM-1 (IC_{50} = 560−2000 nM) and does not inhibit at all adhesion of cells expressing $\alpha4\beta7$ to immobilized MAdCAM-1. However, EMF10 potently inhibits adhesion of cells expressing $\alpha5\beta1$, including K562 cells and guinea pig megakaryocytes, to immobilized fibronectin (IC_{50} = 1−4 nM). Moreover, resting guinea pig megakaryocytes, which express predominantly $\alpha5\beta1$ integrin (*19*), adhere to immobilized EMF10 as extensively as to immobilized fibronectin, and this adhesion is followed by the formation of blebs and pseudopods, suggesting cytoskeletal reorganization. Our experimental data suggests that EMF10 inhibits $\alpha4\beta1$ directly rather than indirectly by altering $\alpha5\beta1$ function. In fact, the inhibitory effect of EMF10 on the adhesion of Jurkat cells (expressing both $\alpha4\beta1$ and $\alpha5\beta1$) to immobilized VCAM-1 was even weaker than its effect on the adhesion of Ramos cells (expressing only $\alpha4\beta1$) to immobilized VCAM-1. However, the inhibitory effects of EMF10 and EC3 on the adhesion of lymphoid cells to immobilized VCAM-1 appear to be mediated by different mechanisms. We have previously shown (*10*) that EC3 competes with monoclonal antibody HP2/1 for the binding epitope on $\alpha4$, and such a competition was not observed in experiments with EMF10 (Figure 4). By the contrast, GRGDSP peptide inhibited adhesion of Jurkat cells to immobilized EMF10, but it had no effect on the adhesion of the same cells to immobilized EC3 (*10*). We propose that EC3 has a high affinity to $\alpha4\beta1$ and $\alpha4\beta7$ integrins, whereas EMF10 mostly affects $\alpha5\beta1$. This was further elaborated studying the expression of LIBS epitope on $\beta1$ subunit of $\alpha5\beta1$ integrin present on K562 cells (Figure 5). EMF10 is the most potent inhibitor of this integrin and also the most potent LIBS inducer, followed by echistatin and EC3. EMF10 did not express LIBS epitope on Ramos cells expressing $\alpha4\beta1$ and deficient in $\alpha5\beta1$ (data not shown).

We have previously suggested, that the KRAMLDGLNDY sequence of subunit B of EC3, with MLD substituting typical RGD motif of disintegrins, represents an epitope recognizing $\alpha4$ integrin (*10*). We identified sequence KKGRGDNLNDY in EMF10A and sequence WPAMGDWNDDY in subunit B. It appears that the selective recognition of $\alpha5\beta1$ integrin by EMF10 depends on both sequences. Two cyclic peptides CKKGRGDNLNDYC and CWPAMGDWNDDYC, patterned on the putative hairpin loop of both subunits of EMF10, inhibited adhesion of K562 cells to immobilized fibronectin with similar potency and at the same concentrations had no effect on adhesion of VNRC3 cells (expressing $\alpha v\beta3$) to immobilized vWF and on the adhesion of A5 cells (expressing $\alpha IIb\beta3$) to fibrinogen. Interestingly, isolated EMF10B expressed much higher anti-$\alpha5\beta1$ activity than isolated EMF10A. It is possible that disruption of S−S bridges during reduction and alkylation interferes more strongly with the activity of RGDNL motif than with the activity of MGDWN motif. A possibility that the WPAMGDWNDDY motif plays a primary role in $\alpha5\beta1$ recognition should be considered. A number of disintegrins containing the RGDN motif in their hairpin loop are strong inhibitors of $\alpha v\beta3$ (*27*, *28*). Although EMF10 is expressing RGDN in subunit A, the inhibitory effect of the whole molecule on $\alpha v\beta3$ and $\alpha IIb\beta3$ is minimal. It can be speculated that the EMF10A hairpin loop is sterically hindered by EMF10B.

Despite of a number of searches to identify $\alpha5\beta1$ antagonists using a phage library (*7*, *8*), biological activity of WPAMGDWNDDY was not identified. An unusual feature of this sequence is the presence of two tryptophans and one methionine that substitutes for arginine. Koivunen's cyclic peptide GACRRETAWAC, which binds specifically to $\alpha5\beta1$, contains one tryptophan (*7*, *8*).

A common feature of monomeric and heterodimeric disintegrins is that they all are strong inducers of LIBS epitopes. In previous studies, we demonstrated that monomeric disintegrins such as echistatin, eristostatin, kistrin, flavoridin, and albolabrin are strong inducers of LIBS epitopes located at the C-terminal region of extracellular domain of $\beta3$ integrin (*13*, *21*, *27*). LIBS activity of monomeric disintegrins is about 4−5 orders of magnitude greater than LIBS activity of short RGDX peptides (*21*), and it seems to be related to the binding affinity of disintegrin to $\alpha IIb\beta3$. Whereas amino acid residues in the disintegrin hairpin loop appear to determine selectivity of these peptides, the C-terminal end of disintegrins appears to be of a similar significance for LIBS induction both in $\alpha IIb\beta3$ and $\alpha v\beta3$ integrin. In this paper, we describe a novel observation that disintegrins express LIBS epitope on $\beta1$ integrin. This was confirmed and elaborated recently by Wierzbicka-Patynowski et al. (manuscript submitted). We demonstrated LIBS effect of EMF10, EC3, and echistatin using K562 cells as a source of $\beta1$ integrin and a monoclonal antibody 9EG7 that recognizes expression of LIBS epitope on this integrin after ligand binding. Eristostatin that binds to $\alpha IIb\beta3$ causes expression of LIBS epitope on this integrin. It does not interact with $\alpha5\beta1$ (*28*), and it does not cause expression of LIBS epitope on K562 cells recognizable by 9EG7. The C-terminus of disintegrins seems to be important in LIBS expression. The molecular model of disntegrins obtained by NMR studies showed localization of C-terminus near active hairpin loop (*21*). This may suggest that C-terminal amino acids support activity of disintegrins and is critical for induction of conformational changes on integrins. We have previously shown that truncated echistatin 1−41, in which this motif is missing, does not induce LIBS epitope in $\beta3$ integrin (*21*). It is noteworthy that EMF10 does not induce LIBS epitope in cells transfected with $\beta3$ integrin in agreement with the contention that ligand recognition by the integrin is a prerequisite for conformational change.

Currently, we are in the process of establishing amino acid sequences and studying biological function of other members of the subfamily of heterodimeric disintegrins including CC5 and CC8 isolated from *Cerastes cerastes* and EC6 isolated

from *Echis carinatus* venom. These three new disintegrins are potent inhibitors of $\alpha5\beta1$ integrins and have a molecular mass between 14 and 15 kDa, as determined by mass spectrometry. The dimeric disintegrin contortrostatin, isolated by Trikha et al. (*29*) and Clark et al. (*30*), also belongs to the same family of proteins.

In conclusion, we identified, isolated and characterized structurally a novel heterodimeric disintegrin EMF10, occurring in the venom of *E. maccmahoni*. This disintegrin, composed of two subunits containing 69 and 64 (or 68) amino acid residues, is an extremely potent and selective inhibitor of $\alpha5\beta1$ integrin. We also identified a novel sequence, CWPAMGDWNDDYC, that may represent the $\alpha5\beta1$ binding site.

ACKNOWLEDGMENT

The authors thank Dr. Mark E. Renz for the generous gift of recombinant VCAM-1; Drs. M. Ginsberg and J. Loftus for CHO cells transfected with αIIb$\beta3$ and $\alpha v\beta3$ integrins; and Dr. A. Garcia-Pardo for RPMI 8866 cells.

REFERENCES

1. Hynes, R. O. (1992) *Cell 69*, 11−125.
2. Hynes, R. O. (1996) *Dev. Biol. 180*, 402−412.
3. Ruoslahti, E. (1996) *Annu. Rev. Dev. Biol. 12*, 697−715.
4. Matter, M. L., Zhang, Z., Nordstedt, C., and Ruoslahti, E. (1998) *J. Cell Biol. 141*, 1019−1030.
5. Zhang, K., Vuori, K., Reed, J. C., and Ruoslahti, E. (1995) *Proc. Natl. Acad. Sci. U.S.A. 92*, 6161−6165.
6. Wary, K. K., Mainiero, F., Isakoff, S. J., Marcantonio, E. E., and Giancotti, F. G. (1996) *Cell 87*, 733−743.
7. Koivunen, E., Gay, D., and Ruoslahti, E. (1993) *J. Biol. Chem. 268*, 20205−20210.
8. Koivunen, E., Wang, B., and Ruoslahti, E. (1994) *J. Cell Biol. 124*, 373−380.
9. Pachter, J. A., Zhang, R., and Mayer-Ezell, R. (1997) *Anal. Biochem. 230*, 101−107.
10. Marcinkiewicz, C., Calvete, J. J., Marcinkiewicz, M. M., Raida, M., Lobb, R. R., Vijay-Kumar, S., Huang, Z. and Niewiarowski, S. (1999) *J. Biol. Chem 274*, 12468−12473.
11. Bazzoni, G., Shih, D.-T., Buck, C. A., and Hemler, M. E. (1995) *J. Biol. Chem. 270*, 2557−25577.
12. Renz, M. E., Chiu, H. H., Jones, S., Fox, J. W., Kim, K. J., Presta, L. G., and Fong, S. (1994) *J. Cell Biol. 125*, 1395−1406.
13. McLane, M. A., Kowalska, M. A., Silver, L., Shattil, S., and Niewiarowski, S. (1994) *Biochem. J. 301*, 429−436.
14. O'Toole, T. E., Loftus, J. C., Du, X., Glass, A., Ruggeri, Z. M., Shattil, S. J., Plow, E. F., and Ginsberg, M. H. (1990) *Cell Regul. 1*, 883−893.
15. Huang, T.-F., Holt, J. C., Lukasiewicz, H., and Niewiarowski, S. (1987) *J. Biol. Chem. 262*, 16157−16163.
16. Wang, S. S. (1973) *J. Am. Chem. Soc. 95*, 1328−1333.
17. Marcinkiewicz, C., Rosenthal, L. A., Mosser, D. M., Kunicki, T. J., and Niewiarowski, S. (1996) *Biochem. J. 371*, 118−124.
18. Bazzoni, G., and Hemler, M. E. (1998) *Trends Biochem. Sci. 23*, 30−34.
19. Schick, P. K., Wojenski, C. M., He, X., Walker, J., Marcinkiewicz, C., and Niewiarowski, S. (1998) *Blood 92*, 2650−2657.
20. Siddiqi, A. R., Perrson, B., Zaidi, Z. H., and Jornvall, H. (1993) *Peptides 13*, 1033−1037.
21. Marcinkiewicz, C., Vijay-Kumar, S., McLane, M. A., and Niewiarowski, S. (1997) *Blood 90*, 1565−1575.
22. Gould, R. J., Polokoff, M. A., Friedman, P. A., Huang, T.-F., Cook, J. J., and Niewiarowski, S. (1990) *Proc. Soc. Exp. Biol. Med. 195*, 168−171.
23. Niewiarowski, S., McLane, M. A., Kloczewiak, M., and Stewart, G. J. (1994) *Semin. Hematol. 31*, 283−300.
24. Calvete, J. J., Wang, Y., Mann, K., Shafer, W., Niewiarowski, S., and Stewart, G. J. (1992) *FEBS Lett. 309*, 316−320.
25. Senn, H., and Klaus, W. (1993) *J. Mol. Biol. 232*, 907−925.
26. Adler, M., Lazarus, R. A., Dennis, M. S., and Wagner, G. (1991) *Science 235*, 445−448.
27. Juliano, D., Wang, Y., Marcinkiewicz, C., Rosenthal, L. A., Stewart, G. J., and Niewiarowski, S. (1996) *Exp. Cell Res. 225*, 2482−2487.
28. Pfaff, M., McLane, M. A., Beviglia, L., Niewiarowski, S., and Timpl, R. (1994) *Cell Adhes. Commun. 2*, 491−500.
29. Trikha, M., De Clerck, Y. A., and Markland, F. S. (1994) *Cancer Res. 54*, 4993−4998.
30. Clark, E. A., Trikha, M., Markland, F. S., and Brugge, J. S. (1994) *J. Biol. Chem. 269*, 21940−21943.
31. Gan, Z.-R., Gould, R. J., Jacobs, J. W., Friedman, P. A., and Polokoff, M. A. (1988) *J. Biol. Chem. 263*, 19827−19832.
32. Dennis, M. S., Henzel, W. J., Pitti, R. M., Lipari, M. T., Napier, M. A., Deisher, T. A., Buntig, S., and Lazarus, R. A. (1990) *Proc. Natl. Acad. Sci. U.S.A. 87*, 2471−2475.
33. Musial, J., Niewiarowski, S., Rucinski, B., Stewart, G. J., Williams, J. A., and Edmunds, L. H., Jr. (1990) *Circulation 82*, 261−273.
34. Scarborough, R. M., Rose, J. W., Hsu, M. A., Phillips, D. R., Fried, V. A., Cambell, M. A., Nannizzi, L., and Charo I. F. (1991) *J. Biol. Chem. 266*, 9359−9362.
35. Shimokawa, K., Jia, L.-G., Shannon, J. D., and Fox, J. W. (1998) *Arch. Biochem. Biophys. 354*, 239−246.

BI9906930